# Ultrafast all-optical switching in a silicon-nanocrystal based silicon slot waveguide at telecom wavelengths

*Alejandro Martínez,[1],* Javier Blasco,[1] Pablo Sanchis,[1] José V. Galán,[1] Jaime García,[1] Emmanuel Jordana,[2] Pauline Gautier,[2] Youcef Lebour,[3] Sergi Hernández,[3] Romain Guider,[4] Nicola Daldosso,[4] Blas Garrido,[3] Jean Marc Fedeli,[2] Lorenzo Pavesi,[4] and Javier Martí[1]*

1. Nanophotonics Technology Center (NTC), Universidad Politécnica de Valencia, Camino de Vera s/n, 46022, Valencia, Spain

2. CEA-LETI, Minatec, 17 rue des Martyrs, Grenoble, France

3.Departament d'Electrònica, Universitat de Barcelona, Carrer Martí i Franquès 1 08028 Barcelona, Spain,

4. Nanoscience Laboratory, Department of Physics, University of Trento, via Sommarive 14, 38122 Trento, Italy

* To whom correspondence should be addressed. E-mail: amartinez@ntc.upv.es

ABSTRACT: We demonstrate experimentally all-optical switching on a silicon chip at telecom wavelengths. The switching device comprises a compact ring resonator formed by horizontal silicon slot waveguides filled with highly-nonlinear silicon nanocrystals in silica. When pumping at power levels about 100 mW using 10 ps pulses, more than 50% modulation depth is observed at the switch output. The switch performs about one order of magnitude faster than previous approaches on silicon and is fully fabricated using complementary metal oxide semiconductor technologies.

Third-order nonlinear effects need to be exploited in order to implement ultrafast (40 Gbit/s and beyond) all-optical functionalities in photonic integrated circuits. Building such all-optical circuits on silicon-on-insulator (SOI) wafers using conventional complementary metal-oxide-semiconductor (CMOS) tools and processes would mean a significant reduction in costs because of the economies of mass manufacturing. However, silicon suffers from a weak ultrafast Kerr coefficient ($n_2$=4x10$^{-14}$ cm$^2$/W at $\lambda$ = 1550nm) and so two-photon absorption (TPA) becomes the dominant nonlinear optical effect at telecom wavelengths.[1] As a result, the generation of free-carriers (FCs) by single or two photon absorption has been demonstrated as an effective means of achieving all-optical switching and modulation.[2-6] Typically, a photonic cavity is used to increase light-matter interaction,[2] which results in a more efficient nonlinear performance. However, the FC-based approach has two important drawbacks: low switching speeds due to the relatively long (~ 1ns) FC recombination time; and low fan-out due to relatively strong light absorption. The introduction of nanometric defects in the silicon waveguide shortens the recombination time to a few tens of picoseconds,[4-6] but simultaneously increases light scattering, i.e. optical losses. Final device performance is thus poor, with few prospects for improvement.

Since in silicon TPA dominates over the Kerr effect at telecom wavelengths, other materials with high Kerr coefficients have to be considered. A main requirement is that the chosen material should also be fully processed in a CMOS foundry to meet the key requirement of mass-manufacturability. From this point of view, silicon nanocrystals (Si-nc) embedded in silica ($SiO_2$), Si-nc/$SiO_2$, is a material which accomplishes both requirements. First, it has been shown that Si-nc/$SiO_2$ displays a high $n_2$ at telecom wavelengths as a consequence of both quantum confinement and dielectric mismatch effects.[7] And second, this material is produced in conventional CMOS foundries by standard methods such as low-pressure chemical vapor deposition (LPCVD) or plasma-enhanced chemical vapor deposition (PECVD). Indeed, silicon nanocrystals are used to manufacture CMOS flash memories.[8]. Since the refractive index of Si-nc/$SiO_2$ is close to that of silica for low silicon content, waveguides made of this material would

not allow for strong field confinement. To overcome this issue, the slot waveguide has been demonstrated to be a suitable way to strongly confine and guide light in a low index medium.[9]

In this work we propose a horizontal silicon slot waveguide filled with Si-nc/$SiO_2$ as a highly Kerr nonlinear medium to achieve ultrafast all-optical switching on silicon. The term horizontal means that the electric field discontinuity that provides a strong field confinement inside the slot occurs at horizontal interfaces and so, quasi transverse-magnetic (TM) polarization must be used. A cross-sectional view of this waveguide is schematically depicted in Fig. 1(a). Compared to the common vertical slot waveguide as originally proposed in Ref. 9, in the horizontal configuration there is no limit for the minimum achievable slot thickness $t_s$ so it can be reduced well below 100nm to minimize the effective area $A_{eff}$ of the guided mode and, as a result, maximize the nonlinear interaction.[10]. For instance, if $t_s$=50nm then the electrical field is strongly confined inside the slot for quasi-TM polarization and resulting in $A_{eff}$=0.06 $\mu m^2$ (see the electric field pattern in Fig. 1(a)).[10] In addition, the horizontal slot can be perfectly filled with the nonlinear material unlike its vertical counterpart, as seen in Fig. 1(b), which shows a scanning electron microscope image of the cross-section of one of the fabricated waveguides. The fabrication process is fully CMOS (details about the fabrication procedure can be found in Ref. 11) and so all-optical circuits based on slot waveguides filled with Si-nc/$SiO_2$ can be entirely manufactured in a microelectronics foundry by use of mainstream processes and tools.

Before fabricating the horizontal slot waveguide circuits, the Si-nc/$SiO_2$ material was deposited onto a transparent silica substrate forming 500 nm layers in order to test their linear and nonlinear properties. The Kerr coefficient $n_2$ as well as the TPA parameter were measured at 1550 nm using the Z-scan technique.[12] A fs laser source was used to differentiate between the Kerr (fast), the free-carriers (slow) and the thermal (even slower) contributions to the $n_2$ coefficient. More details about the experimental measurements can be found in Ref. 7. It was found that, at low optical intensities, the Kerr effect dominates the nonlinear response. The experimentally determined values (maximum) of the Kerr coefficient $n_2$ and the TPA coefficient $\beta$ are shown in Table 1 for both deposition methods: PECVD and LPCVD. It should be noticed that the nonlinear performance strongly depends on silicon excess and the

annealing temperature.[7] However, values of $n_2$ between one and two orders of magnitude higher than in bulk silicon[1] are attainable by properly tailoring the silicon excess, the annealing temperature, and the deposition process.

Previous results were obtained for relatively thick (in comparison with the slot) Si-nc/$SiO_2$ layers, where the nanocrystals are expected to be homogeneously distributed over the whole volume. However, it was not clear if similar conditions (mainly in terms of mean size and homogeneity) would be achieved when depositing the Si-nc/$SiO_2$ in thin (50 nm) slots. An Energy Filtered Transmission Electron Microscopy (EFTEM) analysis of the 50 nm-thick LPCVD slot layer was performed with a 200 kV field-emission Jeol 2010F electron microscope in order to monitor the location and size distribution of Si-nc. The Si-nc contrast in the EFTEM images was enhanced by energetically filtering the electron energy-loss spectra by using a Gatan Image Filter (GIF 2000) around the Si plasmon (placed at 17 eV), which is well separated from the $SiO_2$ plasmon (placed at 22 eV). In this way it was possible to detect the appearance of amorphous clusters inside the oxide matrix and determine their actual size. The results are shown in Fig. 2. It can be observed that the precipitation is uniform and well achieved (Fig. 2(a)). The observed Si-nc have a medium diameter of 2.4 nm (Fig. 2(b)) and are homogeneously distributed. This is mainly because LPCVD proceeds at low deposition so very thin layers with nm-scale control may be deposited with uniform composition over the whole thickness. We should mention that this is more difficult to achieve when using PECVD deposition, which is a faster process and does not provide uniform concentration of Si-nc in thin layers.

We fabricated a very simple and compact photonic structure to demonstrate all-optical switching: a ring-resonator (RR) coupled to a waveguide (see the diagram depicted in Fig. 3(a)). It has been proposed that this switching structure can perform very efficiently with moderate power levels when using slot waveguides filled with Si-nc/$SiO_2$ .[13] The Si-nc/$SiO_2$ material was deposited by LPCVD, which allowed for a higher Kerr coefficient as shown previously. After deposition of SiOx with a 0.17 silicon excess, the material was annealed at 1000°C during 3min30s under pure $N_2$ ambiance to allow for the formation of these Si-nc. The dimensions of the fabricated horizontal slot waveguides were $w$=565nm, $t_1$ = 220nm,

$t_2$ = 252nm and $t_S$ = 50nm. For such dimensions, propagating losses of the waveguides were measured to be of the order of 4 dB/cm.[14] The RR was spaced 250nm from the waveguide and its radius was 20 μm. The transmission spectrum of the fabricated structure in the linear regime for TM-polarized light is shown in Fig. 3(b) (black curve). The observed RR resonance is characterized by a loaded quality factor of 1875 (corresponding to a photon lifetime about 1.54ps inside the cavity) and a 17 dB transmission dip. To test the resonance behavior in the dynamic regime we also measured the optical transmission of a probe signal when a high-power pump signal (1 ps pulses at 10 GHz repetition rate) tuned to an adjacent RR resonance ($\lambda_{pump}$=1557.5nm) was injected into the input waveguide. The pulsed pump signal was generated from a fibre laser with a 10 GHz repetition rate and tunable in the range 1530-1565 nm. At the output of the chip an optical filter was used to remove the remaining pump signal. It is observed in Fig. 3(b) that the resonance dip was clearly red-shifted when the pump power was increased (values of the on-chip peak pump power are indicated). This means that the effective index of the RR is increased, which could be attributed to thermal effects or the Kerr nonlinearity, but not to FC excitation. Additionally, the transmission dip was decreased down to values around 6dB. Since the spectra were recorded with an optical spectrum analyzer that operates by averaging over a temporal interval much larger than the pulse duration, it can be concluded that the red shift is mainly originated by slow thermal effects. This leads us to conclude that the RR must be critically coupled when operating under a nonlinear regime in order to achieve the optimal performance of an all-optical switch. Such a switch would result from a more sophisticated design that should take into account thermal effects – as well as dynamic generation of FCs - inside the RR.

The time response of the switching structure was also measured by using a pump-probe scheme. The pump signal was generated by modulating a 10 GHz pulse train with a certain digital sequence using an electro-optical modulator that was driven by an electrical signal generated by a 40 Gbit/s bit pattern generator. At the modulator output, the pulse width was estimated to be about 10 ps. The modulated signal was amplified using an erbium-doped fiber amplifier. The probe signal was generated by an external cavity laser and was amplified by an erbium-doped fibre amplifier. The polarization of both

signals was controlled independently in order to inject only TM-polarized light into the silicon chip. Both signals were combined before entering the silicon chip. In the experiment, the probe signal was tuned to $\lambda_{CW}$=1544.5nm, which is close to the RR resonance shown in Fig. 3(b). However, the RR resonance is shifted depending on the pump power. This shift depends, as previously argued, on the thermal effects induced by the pump power. Therefore, we could modify the resonance position by controlling the pump power. The time evolution of the output probe signal when the peak pump power at the waveguide input was 150 mW is shown in Fig. 3(c). In this case, the transmission dip due to the RR resonance was close to $\lambda_{CW}$=1544.5nm so transmission is low in the absence of the pump pulse. In the presence of the ultra- short pump pulse, the RR resonance is rapidly red-shifted and a positive pulse is registered at the output. These positive peaks, correspond to positive pulses (digital 1) of the pump signal, have a duration of 11 ps at half-maximum and have an extinction ratio ER = 2.2dB (40% modulation depth). This demonstrates the ultrafast nonlinear response of the all-optical switching structure. Actually, this fast response is due to the Kerr nonlinearity being superimposed on a slow (a few ns) and weak response caused by the excitation of FCs inside the RR. Interestingly, this slow response shows both cumulative effects and long recovery times. The slow response variation is below 1dB for the considered digital sequence. In a real device, this slow effect could be completely avoided by appropriately encoding the digital sequences (e.g. line codes such as 8B/10B)[15] that are widely used to maintain the DC-balance and remove low-frequency detrimental effects in digital communication systems.

We obtained the results shown in Fig. 3(d) by narrowing the recorded time window to that corresponding to a single output pulse at the probe wavelength $\lambda_{CW}$=1544.5nm. The measured output pulse when the on-chip pump peak power was 160mW is shown in blue. In this case, the probe signal is in the RR resonance and, therefore, the transmission increases as the RR resonance is red-shifted due to the pump pulses. An ER=3.6dB (more than 50% of modulation depth) with a 11 ps duration at half-maximum is observed. This considerably overlaps the pump pulse time duration, which is further proof of the instantaneous Kerr effect. When the on-chip peak pump power was reduced to 80mW, the output

pulse shown in red was recorded at $\lambda_{CW}$. In this case, the RR resonance is slightly blue-shifted due to the thermal effects since is higher than the resonance. In both cases, a transient effect that is opposite to the Kerr nonlinearity dynamics is observed at the beginning of the output pulse. This may be attributed to the onset of the excitation of FCs that produces a negative change in the refractive index. However, and in contrast with the behavior observed in silicon wires, the Kerr effect dominates the nonlinear dynamic response of the switching structure so FCs only produce a slow response with an amplitude variation much smaller than the fast variation originated by Kerr. For the sake of comparison, when the probe signal is tuned far from the RR resonance, no switching is observed in the presence of the pump pulse (yellow curve in Fig. 3(d)). Similar experiments performed with quasi-TE polarization (i.e. no field enhancement in the slot region) did not produce any appreciable fast switching effect, and this rules out the role of the silicon strips in the observed effect.

These results lead us to conclude that this all-optical switching structure performs about 10 times faster than other previous silicon switches in which both pump and probe signals are both within the third telecom window.[2-4] In addition, the required on-chip pump power (< 100mW for the red curve in Fig. 3(d)) is also lower than in Refs. 3-4. An ER of the order of those reported in Ref. 2 (~8dB) and Ref. 4 (~9dB) could be also achieved by using a RR with a higher quality factor and designed to perform optimally under dynamic working conditions. Moreover, in our approach both probe and pump signals are placed in the telecom window. In this sense, the presented device also improves other approaches that make use of pump signals within the silicon absorption band (410nm in Ref. 6 or 800nm in Ref. 5) and, therefore, would be useless in a realistic network. The presented result can therefore be considered as a proof-of-concept of ultrafast all-optical switching at telecom wavelengths on a CMOS silicon chip.

It should be mentioned that the slot waveguide could also be filled with other low-index highly-nonlinear materials in order to obtain very good nonlinear performance on a silicon chip. For instance, a vertical slot waveguide filled with a nonlinear polymer ($n_2$ = 1.7×10-13 $cm^2/W$) has been used to demultiplex a 160 Gbit/s signal by means of a four-wave mixing process.[16] This vertical configuration is not straightforward to achieve with CMOS processes because fabrication requires the formation of the

slot using deep ultraviolet lithography (limited to a width of around 120 nm, which is larger than those required to minimize $A_{eff}$)[10] and a subsequent filling of the air slot with nonlinear material (which results in a non-uniform filling and the formation of an air channel when filling with Si-nc)[16]. More importantly, the deposition of polymers is not a typical CMOS process. In addition, the thermal stability of organic materials is poorer than that for inorganic materials, which means that the integration of polymers in CMOS is really a back-end issue as the process has to take place strictly at the end.

In all the measurements, light was injected to and collected from the slot waveguides by making use of lensed fibers. At the chip ends, the slot waveguides have a 3 μm width that was adiabatically reduced to the 500 nm width. This resulted in very high coupling losses (about 10 dB per coupling point). By use of proper coupling techniques, light can be efficiently injected to and extracted from circuits built with horizontal slot waveguides. For instance, an inverted taper can achieve theoretically a 93% coupling efficiency per facet.[17] Grating couplers are not so efficient (a 20% coupling efficiency has been demonstrated experimentally).[18] However, this coupling technique would allow for on-wafer testing, which is a prerequisite in the paths towards mass-scale production.

In summary, we have shown that silicon slot waveguides filled with Si-nc/$SiO_2$ material displays a very fast and efficient nonlinear performance at telecom wavelengths. We have presented the proof-of-concept for ultrafast all-optical switching using Si-nc/$SiO_2$ material as a nonlinear medium. A modulation depth over 50% has been achieved for on-chip optical powers of the order of 100 mW and at speeds about 10 times faster than previous approaches using silicon. The use of a micron-size RR results in a very compact structure with a footprint about 500 $\mu m^2$. From the observed output pulse duration of ~10ps, all-optical switching on silicon at speeds well beyond 40 Gbit/s appears feasible. In contrast to silicon waveguides, the ultrafast Kerr effect dominates over the slower FC-related effects. The photonic structures have been entirely made using CMOS processes and equipment, in contrast to other approaches (e.g. those based on nonlinear polymers that require extra back-end processes). Our results could pave the way to the development of all-optical processing circuits on CMOS.

ACKNOWLEDGMENT. The work was financially supported by the EU through project PHOLOGIC (FP7-IST-NMP-017158).

Figure Captions

Figure 1 (Color online). Description of the nonlinear horizontal slot waveguides. (a) Schematic of the cross-section of the waveguide. The waveguide width is $w$. The lower (upper) strip is made of crystalline (amorphous) silicon and has a thickness $t_1$ ($t_2$). The slot is filled with Si-nc/$SiO_2$ material and its thickness is ts. The whole waveguide is placed over a SiO2 layer and covered by tetra-ethyl-ortho-silicate (TEOS). The computed transverse profile of the electric field for quasi-TM polarization for $t_1$ = $t_2$=220 nm, $t_s$ = 50 nm, $w$ = 500 nm and $x$=0.08 is superimposed. (b) Scanning electron microscope (SEM) image of the cross-section of a fabricated slot-waveguide. Measured dimensions are found on the image ($t_s$=47 nm).

Figure 2. Energy Filtered Transmission Electron Microscopy (EFTEM) characterization of the Si-nc/SiO2 layer deposited by LPCVD inside the horizontal slot waveguide. (a) Image showing a homogeneous Si-nc density; (b) Size distribution of the Si-nc inside the slot layer.

Figure 3 (Color online). All-optical switching structure based on a RR coupled to a waveguide. (a) Scheme of the switching structure showing a SEM image of the RR (radius 20 μm). (b) Transmission spectra of a RR resonance at different peak levels (indicated in the figure) of a pump signal injected at an adjacent resonance ($\lambda_{pump}$ =1557.5 nm). The black curve spectrum was measured by swapping the wavelength of a CW optical signal and recording the power at the output. The other spectra were measured in an optical spectrum analyzer from the amplified spontaneous emission noise coming from the erbium-doped fiber amplifier used to boost the pump signal. The probe wavelength $\lambda_{CW}$ used to obtain the results in (c) and (d) is shown as a vertical dashed arrow. (c-d) Probe-signal time waveform at the output of the switching structure. In (c), the on-chip pump peak power ($P_{pump}$) is 150 mW and $\lambda_{pump}$ =1557.5 nm (corresponding to a RR resonance). In (d), each curve corresponds to different values of $P_{pump}$ and $\lambda_{CW}$ (indicated in the figure).

TABLES

Table 1. Experimentally determined material nonlinear properties for thick (500 nm) Si-nc/$SiO_2$ layers by Z-scan measurements at $\lambda$=1550 nm. For each deposition method, the observed maximum vales of $n_2$ are given. Silicon excess refers to the amount of silicon in the deposited silicon-rich oxide in excess with respect to stoichiometric $SiO_2$.

| Deposition method | $n_2$ ($cm^2$/W) | $\beta$ (cm/GW) | Medium characteristics |
|---|---|---|---|
| PECVD | $4 \times 10^{-13}$ | 5 | 0.08 silicon excess, annealing temperature = 800ºC |
| LPCVD | $2 \times 10^{-12}$ | 50 | 0.17 silicon excess, annealing temperature = 800ºC |

REFERENCES


1. Dinu, M; Quochi. F.; Garcia H. *Appl. Phys. Lett*. **2003**, *82*, 2954.

2. Almeida, V. R.; Barrios, C. A.; Panepucci, R. R.; Lipson M. *Nature* **2004**, *431*, 1081.

3. Preble, S. F.; Xu, Q.; Schmidt, B. S.; Lipson, M. *Opt. Lett*. **2005**, *30*, 2891.

4. Tanabe, T.; Nishiguchi, K.; Shinya, A.; Kuramochi, E.; Inokawa, H.; Notomi, M.; Yamada, K.; Tsuchizawa, T.; Watanabe, T.; Fukuda, H.; Shinojima, H.; Itabashi, S. *Appl. Phys. Lett*. **2007**, *90*, 031115.

5. Waldow, M.; Plötzing, T.; Gottheil, M.; Först, M.; Bolten, J.; Wahlbrink, T., Kurz, H., *Opt. Express* **2008**, *16*, 7693.

6. Preston, K.; Dong, P.; Schmidt, B.; Lipson, M. *Appl. Phys. Lett*. **2008**, *92*, 151104.

7. Spano, R.; Daldosso, N.; Cazzanelli, M.; Ferraioli, L.; Tartara, L.; Yu, J.; Degiorgio, V.; Jordana, E.; Fedeli, J. M; Pavesi, L. *Opt. Express* **2009**, *17*, 3941.

8. Ammendola, G.; Ancarani, V.; Triolo, V.; Bileci, M.; Corso, D.; Crupi, I.; Perniola, L.; Gerardi, C.; Lombardo, S.; DeSalvo, B. *Solid-State Electronics* **2004**, *48*, 1483.

9. Almeida, V. R.; Xu, Q.; Barrios, C. A.; Lipson, M. *Opt. Lett.* **2004**, *29*, 1209.

10. Sanchis, P.; Blasco, J.; Martínez, A.; Martí, J. *J. Lightwave Technol.* **2007**, *25*, 1298.

11. Jordana, E.; Fedeli, J. M.; Lyan, P.; Colonna, J.P.; Gautier, P.; Daldosso, N.; Pavesi, L.; Lebour, Y.; Pellegrino, P.; Garrido, B.; Blasco, J., Cuesta-Soto, F.; Sanchis, P. *Proceedings of IEEE International Conference on Group IV Photonics (Tokio, Japan)*, **2007**, 222.

12. Sheik-Bahae, M.; Said, A. A.; Wei, T. H.; Hagan, D. J.; Van Stryland, E. W. *IEEE J. Quantum Electron.* **1990**, *26*, 760.

13. Barrios, C. A. *Electron. Lett*. **2004**, *40*, 862.

14. Guider, R.; Daldosso, N.; Pitanti, A.; Jordana, E.; Fedeli, J.-M.; Pavesi, L. *Opt. Express* **2009** *17*, 20762.

15. Widmer A. X., Franaszek P. A., *IBM Journal of Research and Development* **1983**, 27, 440.

16. Koos, C.; Vorreau, P.; Vallaitis, T.; Dumon, P.; Bogaerts, W.; Baets, R.; Esembeson, B.; Biaggio, I.; Michinobu, T.; Diederich, F.; Freude, W.; Leuthold, J. *Nature Photon*. **2009**, *3*, 216.

17. Galan, J.V.; Sanchis, P.; Blasco, J.; Martinez, A.; Marti, J. *Opt. Comm.* **2008,** *281*, 5173.

18. Galan, J. V.; Blasco, J.; Sanchis, P.; Martinez, A.; Marti, J.; Fedeli, J. M.; Jordana, E.; Gautier, P.; Perrin, M. **Proceedings of IEEE International Conference on Group IV Photonics** (Sorrento, Italy), **2008**, 105.

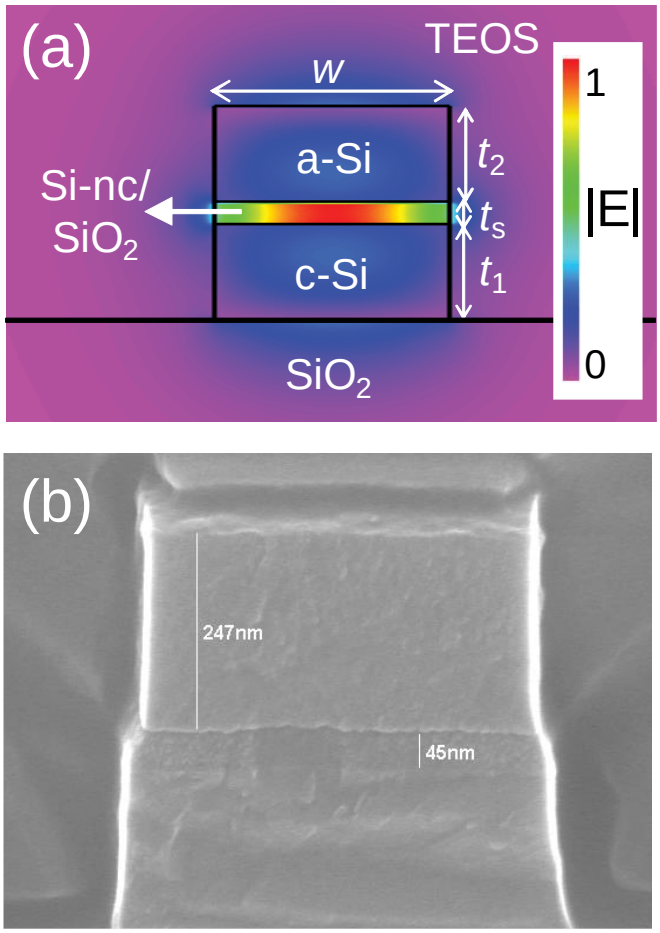


Figure 1

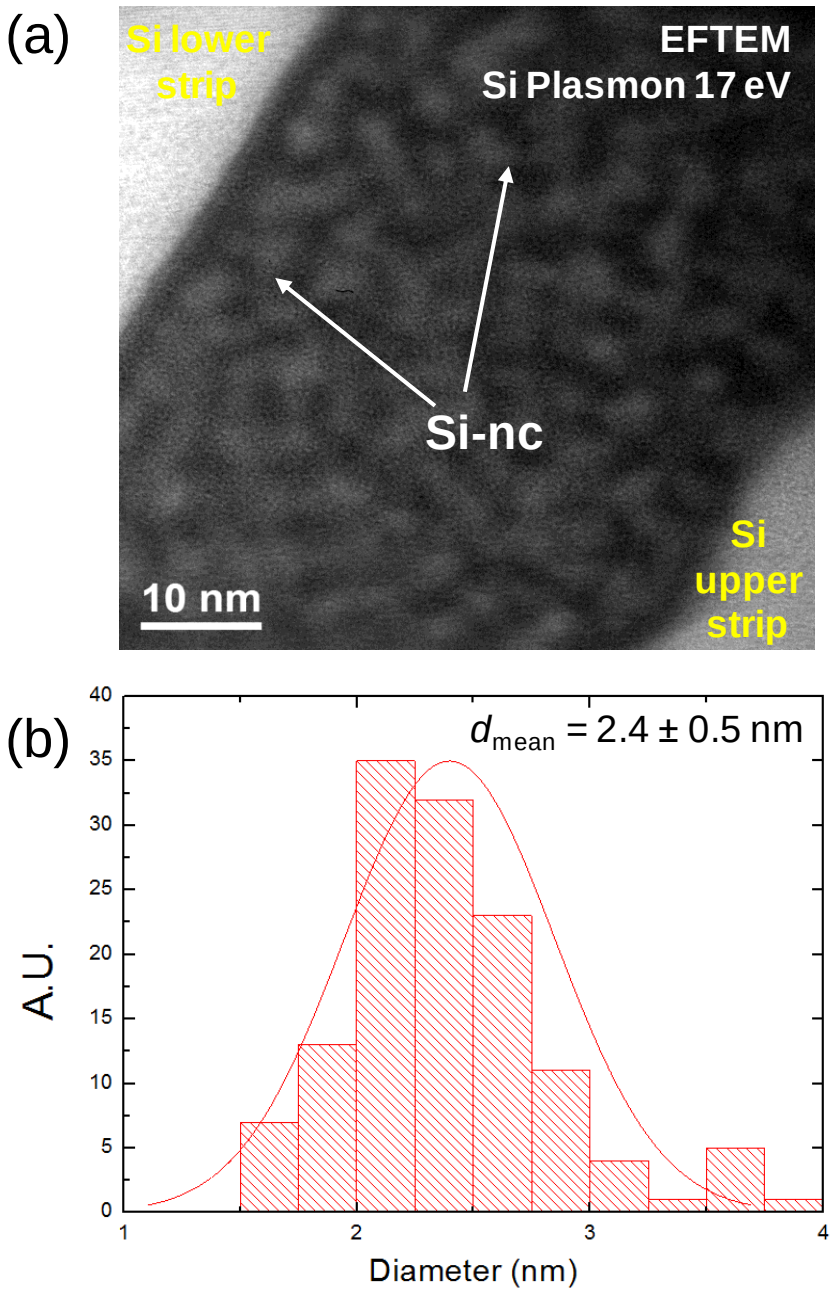
(a)
Si lower strip
EFTEM
Si Plasmon 17 eV
Si-nc
10 nm
Si upper strip
(b)
$d_{mean}$ = 2.4 ± 0.5 nm
A.U.
Diameter (nm)
0
5
10
15
20
25
30
35
40
1
2
3
4

Figure 2

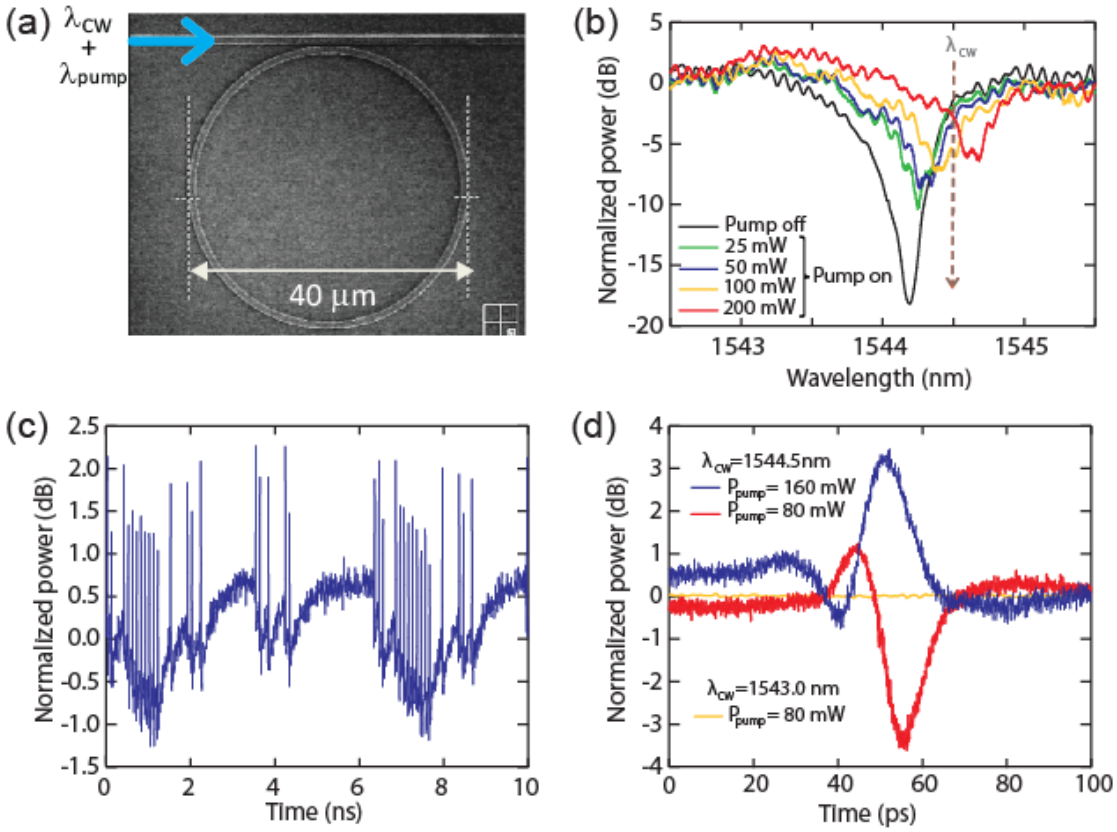
(a)
λCW
+
λpump
40 μm
(b)
Normalized power (dB)
λCW
Pump off
25 mW
50 mW
100 mW
200 mW
Pump on
Wavelength (nm)
(c)
Normalized power (dB)
Time (ns)
(d)
Normalized power (dB)
λCW=1544.5nm
PPump= 160 mW
PPump= 80 mW
λCW=1543.0 nm
PPump= 80 mW
Time (ps)

Figure 3